Materials Science Forum
ISSN: 1662-9752, Vol. 1187, pp 55-62
doi:10.4028/p-3Tuj2F

Submitted: 2025-12-23
Revised: 2026-02-24
Accepted: 2026-02-24
Online: 2026-04-17

Analysis of Connection Geometries for Segmented Stator Cores Machined with Laser Beam Cutting

Florian Hoffmann[1,a*], Philipp Plänitz[1,b], Alexander May[1,c], Florian Winkler[2,d], Markus Barth[2,e], Sören Majcherek[3,f] and Matthias Hackert-Oschätzchen[1,g]

[1]Chair of Manufacturing Technology with Focus Machining, Faculty of Mechanical Engineering, Otto von Guericke University Magdeburg, Universitätsplatz 2, 39106 Magdeburg, Germany

[2]TEPROSA GmbH, Paul-Ecke-Straße 6, 39114 Magdeburg, Germany

[3]Brandenburg University of Applied Sciences, Magdeburger Straße 50, 14770 Brandenburg an der Havel, Germany

[a]florian.hoffmann@ovgu.de, [b]philipp.plaenitz@ovgu.de, [c]alexander2.may@st.ovgu.de, [d]florian.winkler@teprosa.de, [e]markus.barth@teprosa.de, [f]soeren.majcherek@th-brandenburg.de, [g]matthias.hackert-oschaetzchen@ovgu.de (*corresponding author)

Keywords: non-conventional manufacturing, electric motors, stator segmentation

Abstract. Current developments in the transition to renewable energy and the electrification of mobility are leading to higher demands with regard to resource efficiency in the production of electric motors. One current trend is the segmentation of the stator pack, which enables higher material utilization and novel assembly processes. In this paper, different connection geometries for individually stacked stator segments are examined. Experiments were conducted by laser beam cutting and stacking of samples with different segmentations and connection geometries. Afterwards the geometric dimension and tolerances are compared with an unsegmented stator. Furthermore, the impact of the additional connections on the mechanical behavior under load are investigated using Finite Element Analysis. The required force to join segments across different connection geometries ranges from 462 N to 1875 N, while the cylindricity of segmented stator cores spans from 33 µm to 59 µm, compared to 40 µm for the unsegmented sample. Simulation results show that the elastic strain on the connections is largely influenced by the size of air gaps between segments, as well as the geometry and number of segments.

Introduction

Stator cores are manufactured by stacking and bonding thin sheets of electrical steel. For high-volume productions, punching is a cost-effective process. For prototyping or stators with large dimensions, laser beam cutting is also commonly used [1, 2]. The surface of the electrical steel sheets has a protective coating that provides corrosion resistance and electrical insulation. For joining the steel sheets into stator packs there are multiple established methods [1, 3]. Laser welding of the sheets on the outer circumference of the stator yoke or the stamping of an interlocking contour on the surface are simple and cost-effective methods, but they cause electrical contact between the steel sheets, which leads to higher eddy current losses. An alternative joining method is the usage of an adhesive coating to create a bond over the entire surface and maintain the electrical insulation [4].

Segmentation of the stator core offers new opportunities for manufacturing. In addition to a higher material utilization of the electrical steel, the complexity of the winding process can be reduced, while at the same time achieving higher slot fill factors [5]. The targeted use of grain-oriented electrical steel can increase the efficiency of the electrical motor further [6]. However, the additional joining process of the segments and the effects of segmentation regarding the mechanical and electromagnetical properties of the stator core must be considered.

Koshoo et al. conducted an extensive review of current research on the subject of stator and rotor segmentation [6]. Besides a discussion about the advantages and drawbacks of segmentation, different segmentation and manufacturing methods are presented. The influence of cut edges produced with different manufacturing processes on the magnetical properties of the electrical iron is

discussed in multiple publications. Experiments show decreased permeability in the areas near the cut edges [2], and FEM models, which take those cut edge effects into account, are presented [7, 8]. The introduction of additional cut edges through stator segmentation lowers the effective permeability, which causes less magnetic flux compared to an unsegmented stator.

Another phenomenon with implications on efficiency is increased magnetostriction caused by mechanical stress [9]. For example, compressional stresses introduced with shrink fitting the stator into a housing can have a significant impact on the B(H) curve and iron losses of the stator. Local stresses can be increased further with segmentation. In [10], the stress dependent iron losses are examined on a segmented lamination core. Variation of the surface roughness of the segment interfaces show that increased roughness leads to a lower slope of the B(H) curve. The results also show increasing iron losses with higher compressive stress.

This paper examines the manufacturing of segmented stator cores machined with laser beam cutting. Experiments were conducted with different connection geometries and number of segments. After the joining process, the form and shape tolerances are compared to a non-segmented sample. Furthermore, simulation models were developed for the joining process of the segments and for the mechanical stresses to which the stator is subjected during operation. While the primary opportunities are higher material utilization of electrical steel and higher slot fill factors through novel winding techniques, the aim of this study is to evaluate the new challenges arising from stator segmentation.

Experimental Setup

High precision laser beam cutting with a fiber laser (*Kimla PowerCut*) was employed in the manufacturing of the stator cores. The Electrical steel used is M235-35A [11] with a nominal thickness of 0.35 mm and a Backlack coating for adhesive bonding of the steel sheets. Fig. 1a) shows the benchmark geometry used in the experiments. This geometry represents a simplified stator design with 12 slots that includes additional grooves on the outer circumference for enhancing the alignment of sheets during the stacking process. 150 sheets are stacked and bonded in an oven with a temperature of 205 °C for 2 hours in a housing that provides continuous pressure on the lamination stack.

The segmentation type chosen for the experiment is the splitting of the back iron along the slot. Fig. 1b-d) display the investigated connection geometries. These geometries were derived from literature [12] and adapted to the stator dimensions. The interlocking geometries are designed with an air gap of 20 µm, except for the front surfaces of the dovetail (Fig. 1c) and the T-Form (Fig. 1d), which feature an air gap of 100 µm. Each segment is individually stacked and bonded, with manufacturing tolerances of each geometry being measured prior to the joining process. A total number of 10 stator cores was produced, including an unsegmented reference and variations with the three connection geometries. Each connection geometry is examined with two, three and four segments per stator ring.

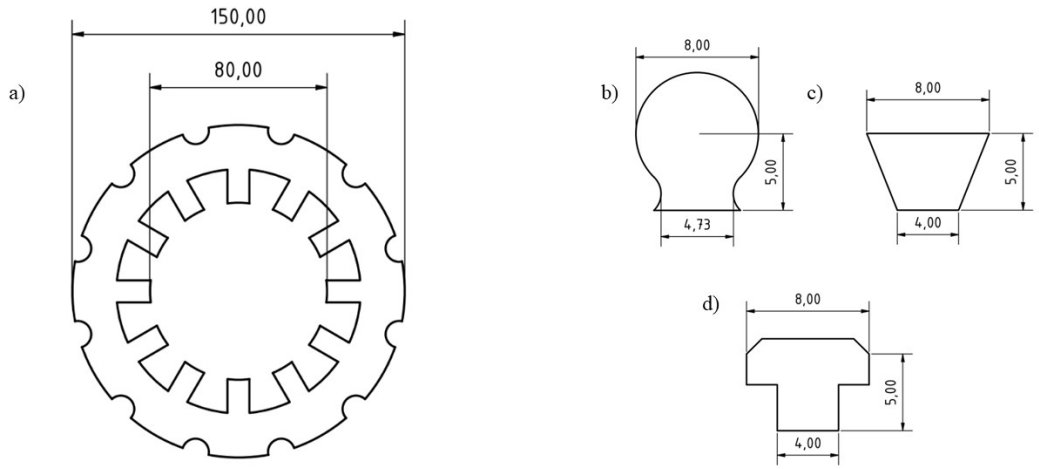

Fig. 1. Benchmark geometry of a) the unsegmented stator and chosen connection geometries: b) Circle, c) Dovetail and d) T-Form

The joining process of the segments is realized with a manually actuated press. The setup is illustrated in Fig. 2. At first the segments are joined a few millimeters with a soft-faced hammer. Then the press is used to fully join the segments. A copper plate between piston and segment is applied to protect the surface, and the joining pressure is monitored during the process.

Fig. 2. Joining process of a quarter-segmented stator with T-Form connection geometry

Following the joining process, the dimensional accuracy of the samples was evaluated using a coordinate measuring machine. By probing the teeth heads, both the roundness and cylindricity of the inner diameter were measured. This measurement is crucial as the accuracy of the inner diameter significantly affects the uniformity of the air gap between the stator and rotor. Such uniformity is vital as it greatly influences the motors operational characteristics. In addition, the flatness of the upper surfaces and the lower surfaces was measured to estimate misalignment of the laminations.

Simulation Model

The simulation models were developed using *COMSOL Multiphysics*. A 3D model was employed to replicate the joining process of the segments, while a 2D model was used to simulate the mechanical stresses during motor operation. The geometries shown in Fig. 1 were transferred to the models. Sharp edges on the stator and at the connection geometries were replaced with fillets in order to prevent the occurrence of singularities during simulation. A fully parametric design allows switching between different connection geometries and number of segments. The simulation models were further extended by two additional connection geometries, illustrated in Fig. 3. On the left, the L-shaped connection geometry is depicted, combined with a single-tooth segmentation that is also implemented in the 2D simulations. On the right, Fig. 3b) shows the 3D model with a rectangular connection geometry and quarter segmentation. To reduce computational effort, the neighboring segments adjacent to the one being pressed down are cut off in the 3D model.

3D Model. The purpose of the three-dimensional model is to analyze the stresses within the joints during the joining process. Experimental observations indicate a linear increase in the force required to displace the segment. This suggests that friction provides the main source of resistance. As a simplification, the laminated stator core is represented as a single solid body, while the surface roughness of the connection interfaces is characterized by a friction coefficient μ. This coefficient is derived from the measured forces during the experiments and can be used to approximate the joining forces required for the connection geometries that were not tested in the experiments.

For the simulation, the quarter segmentation illustrated in Fig. 3b) is selected. The central segment is displaced upward by 5 mm relative to the neighboring segments. The joining process up to this point is not simulated in order to keep the computational effort within reasonable limits. The maximum forces occur at the end of the joining process, and the preceding friction forces can be linearly extrapolated. For the mesh configuration, uniform triangle-elements with an element size of

0.3 mm were applied to the connection surfaces, while the rest of the volume was meshed with tetrahedron-elements.

2D Model. The two-dimensional simulation model is used to compare the stresses and deformations of segmented and unsegmented stator cores. An adaptive Triangle-Mesh was used for the model, with element-sizes ranging from 0.015 mm at the segment connections to 2 mm in uncritical areas. For the stator, an application as a traction machine with concentrated windings and characterized by high torque was assumed. A load case was defined in which a tangential reaction force corresponding to a torque of 500 Nm is applied to two opposing tooth pairs belonging to a single electrical phase of the motor. This represents an extreme scenario, as in reality the torque is generated by more than one electrical phase at any given time. This load was combined with a fixed constraint on the outer circumference of the stator.

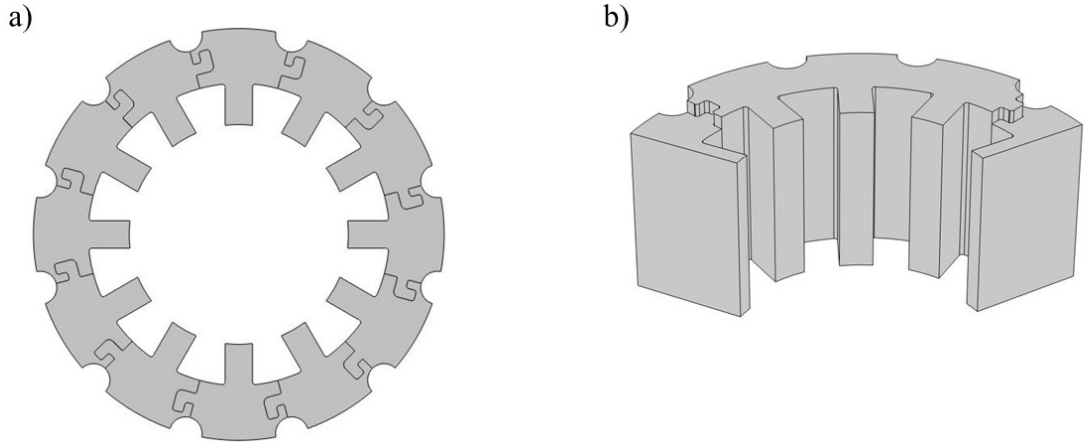

Fig. 3. Simulation models with additional connection geometries. a) L-Form with single tooth segmentation in 2D model, b) Rectangle-Form with quarter-segmentation in 3D

In a second simulation, the stresses induced by a press-fit assembly of the stator into a housing were examined. A radial force was applied to the outer circumference by defining a pre-tensioned spring, while tangential displacement at the outer boundary remains constrained. Aluminum was specified as the housing material, and the spring constant k is derived from the material data, considering an interference of 50 µm. The values used for the material properties are listed in Table 1.

Table 1. Material properties for the simulation models

Material property	Symbol	Electrical Steel (M235-35A)	Housing Material (Al)
Young's Modulus	E	175 [GPa]	200 [GPa]
Poisson's ratio	ν	0.3	0.29
Density	ρ	7600 [kg/m³]	2700 [kg/m³]

Results

Measuring the dimensions of the connection geometries before the stacking process showed an average deviation of 9.1 µm and 9.2 µm for the dovetail and T-shaped connections, respectively. The deviation of the circular geometry was higher, at 17.8 µm. Individual packing of the segments caused additional deviations in segment height due to variations in clamping pressure, as well as temperature and time in the oven. A maximum height difference of 0.27 mm between two corresponding segments was measured.

During the joining process, the hydraulic pressure applied by the press was recorded. The joining force for different connection geometries was derived from the measured pressure and the averages of the samples with the same geometry were calculated. The values listed in Table 2 were measured when joining the final segment to complete the stator ring, where two connections were engaged

simultaneously (see Fig. 2). The lowest force of 462 N was required for the dovetail geometry, followed by the circular geometry with 1184 N and the T-shaped connection with 1875 N. Joining processes with a single connection engaged showed average joining forces approximately three times lower. The form deviations of the connection geometries and slight displacements of the steel sheets during stacking are presumed to be the primary causes of friction, even though the nominal dimensions of the connections provide a clearance of 20 µm.

The joining forces calculated with the 3D model are listed in the right column of Table 2. A representative coefficient of friction μ of 0.138 and an interference fit of +1 µm were determined in order to reproduce the joining forces of the T-shaped geometry measured in the experiments. The deviation between experiment and simulation is 2 N and 71 N for the T-Form and dovetail geometry respectively. For the circular geometry a significantly higher force of 1184 N was observed during the experiments compared to 244 N calculated with the simulation model. This difference could be attributed to the larger form deviation of the circular connection geometry observed in the produced samples, which were not considered in the simulation. Another aspect not represented by the friction based model are offsets between the sheet layers that can lead to shearing and tilting during the joining process.

Table 2. Average Force for joining of segments

Connection geometry	Joining Force – measured [N]	Joining Force – calculated [N]
Circle	1184	244
Dovetail	462	533
T-Form	1875	1877
Rectangle	-	318
L-Form	-	1048

After assembly, the dimensional accuracy of the inner diameter was assessed. Fig. 4a) shows the roundness, measured at 12 points at mid-height. With one exception, the diameter of the fitted circle increases with segmentation. The roundness, defined as the total deviation from the fitted circle (depicted with the error bars), amounts to 26 µm for the unsegmented stator and ranges between 13 µm and 50 µm for the segmented variants. The cylindricity of the inner diameter, determined from measurements in 5 different planes, is illustrated in Fig. 4b). The deviation from the ideal cylindrical shape increases from 40 µm for the unsegmented stator to between 52 µm and 59 µm for the samples with two segments, but decreases with a higher number of segments. Among all connection geometries, the T-shaped configuration exhibits the lowest overall values.

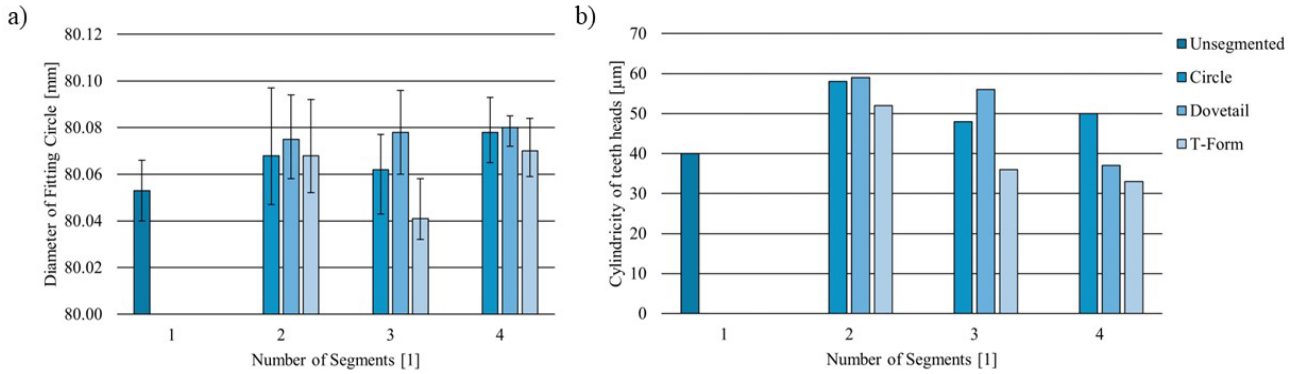

Fig. 4. Form deviation of the stator's inner diameter. a) Roundness at half height, b) Cylindricity

For the results of the 2D simulation, the T-shaped geometry is chosen to present the two load cases in detail before comparing the connection geometries. Fig. 5a) shows the joined experimental sample, while Fig. 5b) and 5c) illustrate the 2D simulation model under two different load cases. In Fig. 5b), a tangential force is applied to the stator teeth near the segment connection. The red arrows indicate the force direction, and the surface coloration corresponds to the von Mises stress in the material. The

roots of the stator teeth experience the maximum stress in this load case, while the displacement of the connection surfaces is less than 1 µm for all geometries. The second load case, simulating a shrink fit, is depicted in Fig. 5c). The stress color scale is adjusted for the overall higher stresses compared to the first load case. Critical areas regarding stress, besides the connection points, include the inner ring of the stator and the round grooves along the outer circumference. The maximum contact pressure is 314 MPa for the T-shaped geometry, which is the highest value of the tested geometries. The dovetail connection showed the lowest maximum contact pressure of 160 MPa.

The simulation model assumes linear elastic and isotropic material properties. Because the difference between the yield point of the electrical steel (see Table 1) and the calculated stresses is sufficiently high, the exclusion of plastic deformation in the model can be considered to be legitimate. The isotropic material properties on the other hand ignore the lamination stack in the perpendicular plane and the influence of the rolling direction on the electrical steel. It was presumed that both have little influence on the considered load cases.

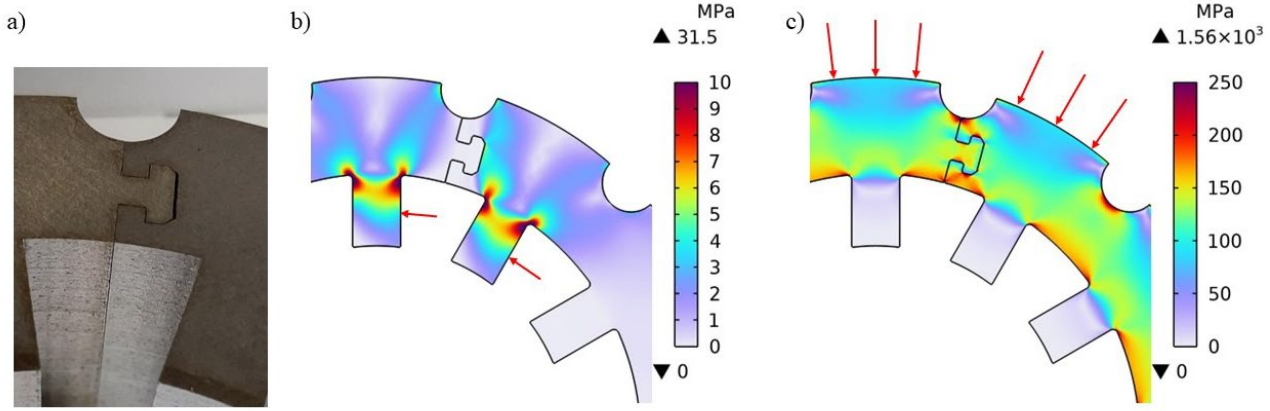

Fig. 5. Segmented stator core with T-Form connection. a) experimental sample, b) simulation model with tangential load on teeth, c) simulation model with radial load on outer circumference

To compare the different connection geometries, the elastic strain energy density W_{el}, integrated over the arc length of the connection, is illustrated in Fig. 6. These values were calculated with the 2D simulation model and pertain to the second load case. In addition to the variations in segmentation and connection geometries, the air gap between tongue and groove was varied at 1 µm, 10 µm, and 20 µm. With the exception of the L-shaped connection, the strain energy density decreases with a higher segment count and wider gaps between segments.

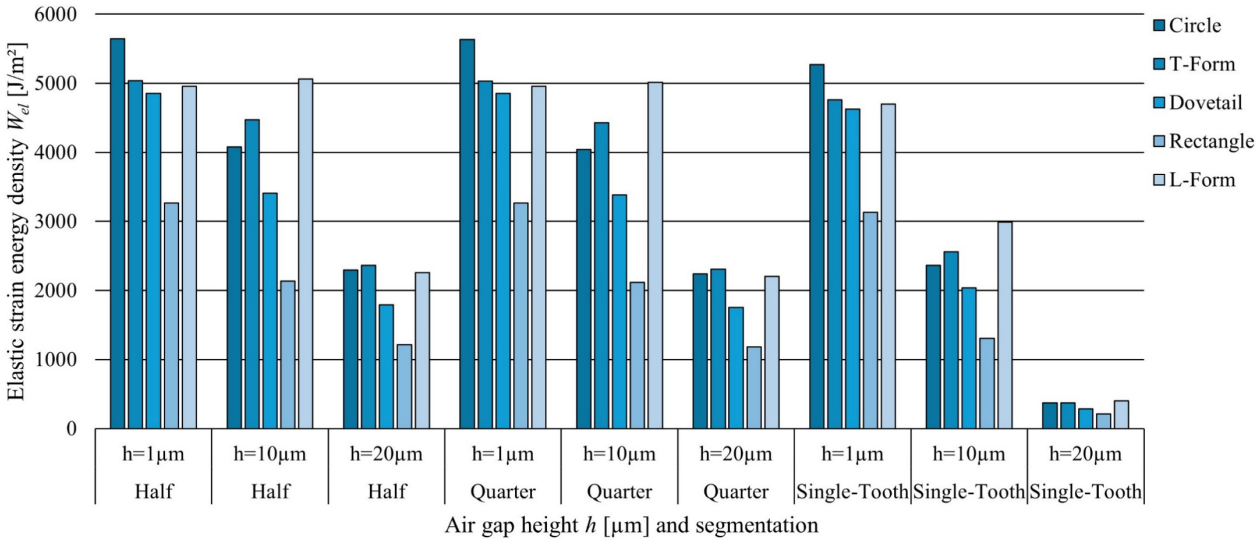

Fig. 6. Elastic strain energy density in the connection for different connection geometries, segmentations and air gap heights

For the L-shaped geometry, increasing the air gap from 1 µm to 10 µm leads to a slight increase in strain energy density for both the half and quarter segmentation. The rectangular geometry exhibits the lowest overall strain energy density, with values between 33 % to 58 % lower compared to the other geometries.

Summary

In this study, the influence of various connection geometries on the mechanical and structural properties of segmented stator cores in electric traction machines was examined. Experimental data revealed an initial increase in form deviations regarding roundness and cylindricity upon segmentation. However, with a higher number of segments, these deviations decreased, eventually equaling or falling below those of the unsegmented stator sample.

By employing both two-dimensional and three-dimensional simulation models using *COMSOL Multiphysics*, the joining forces and stress distributions in different connection geometries were analyzed. Assuming friction as the main component in the force required to join segments, a simulation model was developed to replicate the experimentally recorded joining forces and estimate the forces for new connection geometries. Due to greater form deviations in the circular connection geometry, the average joining force for experimental samples was approximately five times higher than the simulated results.

The 2D simulations provided insights into stress distribution under various loads. Stress induced by rotor torque was considered noncritical, while simulations of shrink-fitting the stator into a housing indicated average stress levels up to a hundred times higher in a single-tooth segment. Increasing the number of segments and larger air gaps between them can reduce strain in the connection points by up to 93 %, but at the expense of dimensional accuracy. Among the different connection geometries, the circular form exhibited the highest elastic strain energy density, while the rectangular shape displayed the lowest.

Acknowledgments

This project is funded by the State of Saxony-Anhalt with funds from the European Union under the European Regional Development Fund under the project number ZS/2024/06/187997.

References

[1] E. Lamprecht, Der Einfluss der Fertigungsverfahren auf die Wirbelstromverluste von Stator-Einzelzahnblechpaketen für den Einsatz in Hybrid- und Elektrofahrzeugen, 2014

[2] Z. Gmyrek, F. Graffeo, S. Vaschetto, A. Cavagnino, Measurements and Modeling of Iron Losses in Guillotine and Laser Cut Soft-Magnetic Sheets. *IEEE IAS*, *6* (2025) 663–675

[3] A. Schoppa, J. Schneider, C.-D. Wuppermann, T. Bakon, Influence of welding and sticking of laminations on the magnetic properties of non-oriented electrical steels. *Journal of Magnetism and Magnetic Materials* (2003).

[4] R. Pugstaller, G.M. Wallner, B. Strauß, R. Fluch, Advanced characterization of laminated electrical steel structures under shear loading. *Journal of Adhesion*, *95*(9) (2019) 834–848

[5] A.M. EL-Refaie, Fractional-slot concentrated-windings synchronous permanent magnet machines: Opportunities and challenges. *IEEE Transactions on Industrial Electronics*, *57*(1) (2010) 107–121

[6] B. Khoshoo, A. Aggarwal, S. Foster, A Review of Segmented Stator and Rotor Designs in AC Electric Machines: Opportunities and Challenges, *Eng*, *6*(1) (2025)

[7] M. Garmut, M. Petrun, Influence of stator segmentation on iron losses in PMSMs for traction applications. *COMPEL*, *41*(2), (2022) 644–658.

[8] J. Rens, S. Jacobs, L. Vandenbossche, E. Attrazic, Effect of Stator Segmentation and Manufacturing Degradation on the Performance of IPM Machines, Using iCARe® Electrical Steels. *World Electric Vehicle Journal*, *8*(2) (2016) 450–460

[9] R. Raj, T. Lindberg, Z. Lin, D. Singh, K. Bergsro, T. Thiringer, Characterizing the Effect of Shrink Fitting of Stator Housings on Electric Vehicle Performance. *IEEE Transactions on Energy Conversion* (2025)

[10] Y. Zhu, B. Mecrow, G. Atkinson, X. Deng, G. Liu, Stress-dependent Iron Loss in Segmented Laminations Considering Surface Roughness. *ICEM 2024*

[11] DIN EN 10106:2015, Cold rolled non-oriented electrical steel strip and sheet delivered in the fully processed state

[12] T. Albrecht, C. Gursel, E. Lamprecht, T. Klier: Joining techniques of the rotor segmentation of PM-synchronous machines for Hybrid drives. *EDPC*, IEEE, 2012 — ISBN 978-1-4673-3008-4, pp. 1–8